Supporting Information

Subissi et al. 10.1073/pnas.1323705111

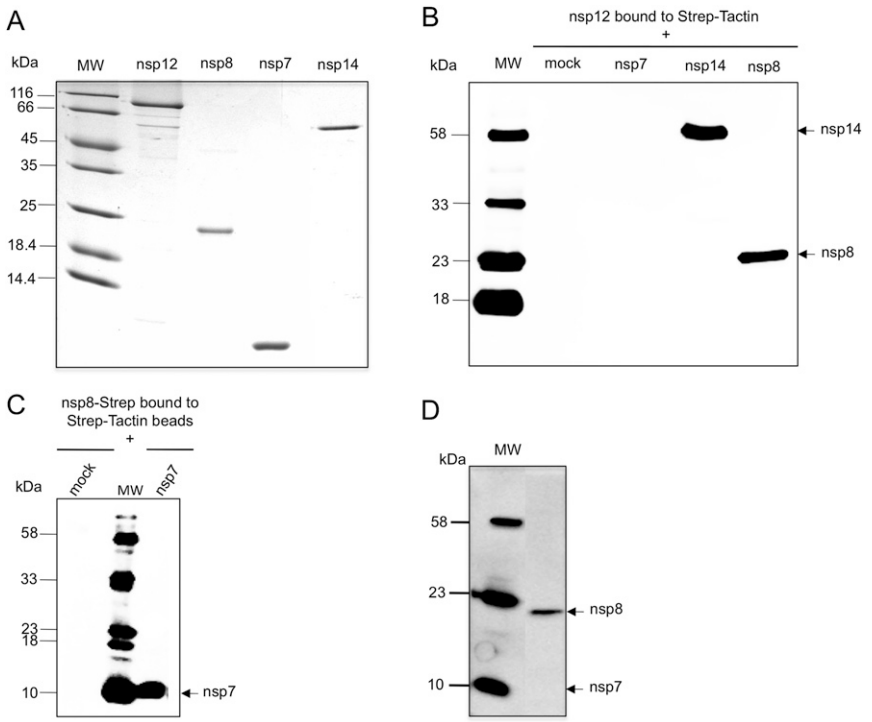

Fig. S1. Nsp8 and nsp14 bind to nsp12, unlike nsp7. Recombinant SARS-CoV proteins carrying affinity tags were expressed in *Escherichia coli* and purified as described in *Materials and Methods*. The C terminus of nsp12 was Strep-tagged, and a hexahistidine tag was added at the C terminus of nsp7 and nsp8 and at the N terminus of nsp14. (*A*) Purified nsp12, nsp8, nsp7, and nsp14 proteins were analyzed by SDS/PAGE (12%) and visualized by Coomassie blue staining. (*B*) Pull-down assays to study the interaction of nsp12 with nsp7, nsp14, and nsp8. Nsp12 was bound to Strep-Tactin beads and incubated without protein (mock) or with 15 μg of nsp7, nsp14, or nsp8. Bound proteins were separated by SDS/PAGE and visualized by immunoblotting with an anti–His_5-HRP antibody. (*C*) Pull-down assay to study nsp7/nsp8 interaction. This time, nsp8 carrying a Strep-tag at its N terminus (nsp8-Strep) and was bound to Strep-Tactin beads, which were incubated without protein (mock) or with nsp7 (15 μg). Detection of nsp7 was performed as in *B*. (*D*) Nsp12 was incubated with an equimolar ratio of nsp7 and nsp8 proteins. Nsp12 and bound partners were purified by use of Strep-Tactin beads, separated by SDS/PAGE, and visualized by immunoblotting with an anti–His_5-HRP conjugate antibody. Molecular weights (MW) are indicated on the *Left* of each panel.

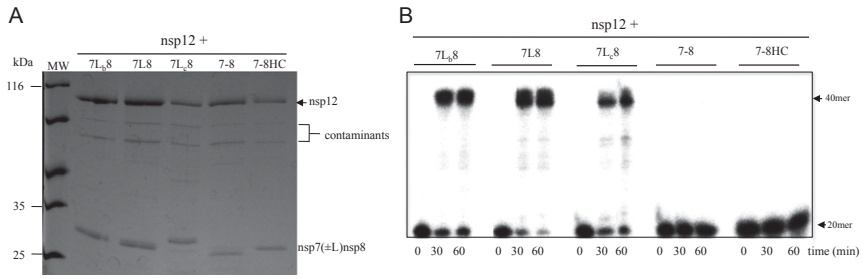

Fig. S2. Effect of different nsp7–nsp8 precursor forms on polymerase activity. (*A*) Strep-nsp12 was copurified with different nsp7–nsp8 fusion protein forms: 7L$_b$8, 7L8 7L$_c$8, where L is an amino acid linker of different lengths (GSGSGS, HHHHHH, and HHHHHHGSGSGS, respectively) added between the nsp7 C-terminal end and the nsp8 N-terminal end; 7–8: "natural" precursor form of nsp7/nsp8; 7–8HC: precursor form with six histidines at the nsp8 C-terminal end. All nsp7/nsp8 protein forms bind to nsp12. After purification on Strep-Tactin beads, the proteins were separated on 12% SDS/PAGE, and protein complexes formed between nsp12 and the different nsp7–nsp8 fusion proteins were visualized by Coomassie blue staining. (*B*) RNA primer extension assays with the five complexes shown in *A*. Purified complexes were incubated together with LS2*/LS1 RNA template in presence of 500 μM of each NTP. The reaction products, collected after the indicated time, and the RNA products were separated on 20% PAGE/7 M urea followed by autoradiography. Primer conversion rates (at 60 min): 42% for 7L$_b$8/12; 84% for 7L8/12; 51% for 7L$_c$8/12; and 0% for both 7–8/12 and 7–8HC/12, clearly indicating that nsp7–nsp8 natural precursor is not functional, as reported in ref. 1.

1. Deming DJ, Graham RL, Denison MR, Baric RS (2007) Processing of open reading frame 1a replicase proteins nsp7 to nsp10 in murine hepatitis virus strain A59 replication. *J Virol* 81(19): 10280–10291.

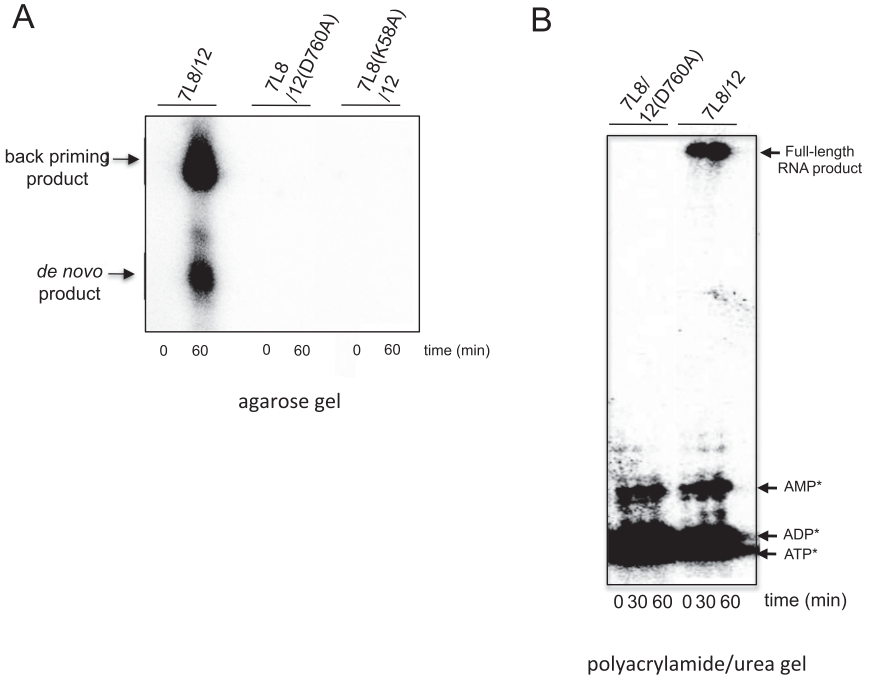

Fig. S3. Nsp8 does not synthesize small oligomers in the context of the 7L8/12(D760A) complex. (*A*) De novo polymerase assays were performed using complexes containing either WT nsp12 (7L8/12) or an active-site knockout of nsp12 [7L8/12(D760A)] or nsp8 [7L8(K58A)/12]. Assays contained 500 nM of each protein complex, 500 nM of 3R RNA template, and a mix of GTP, UTP, and CTP (500 μM each), as well as 50 μM ATP and 0.17 μM [α-^{32}P]ATP (0.5 μCi/μL). Reactions were stopped after 60 min, and products were analyzed by denaturing agarose gel electrophoresis and autoradiography. (*B*) To visualize putative small oligomers, de novo polymerase assays were performed as above using either 7L8/12 or 7L8/12(D760A), but the products were resolved on 14% polyacrylamide/7 M urea gel, and autoradiography. The polymerase assay buffer used is described in *Materials and Methods*, with the addition of 4 mM Mn^{2+}. The positions of residual ^{32}P-labeled (*) ATP, ADP, and AMP are indicated on the *Right* of the autoradiograph.

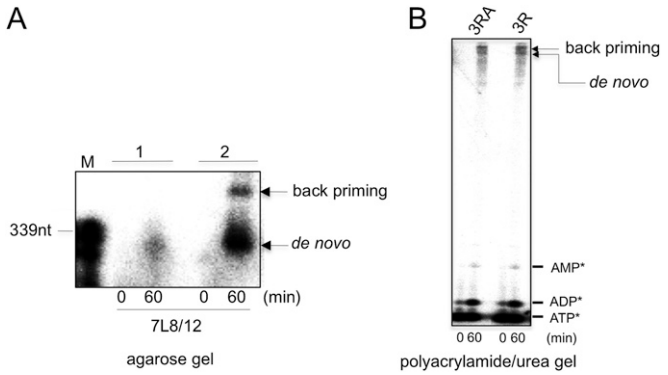

Fig. S4. Polymerase activity of the 7L8/12 complex on different RNA templates. (*A*) The 3R RNA was oxidized using 2.5 mM lithium periodate followed by reduction with 2.5 mM sodium borohydride as described in ref. 1. The 7L8/12 protein complex (500 nM) was incubated with 500 nM of chemically blocked 3R (lane 1) or untreated 3R (lane 2) in the presence of 500 μM GTP, UTP, CTP, 50 μM ATP, and 0.17 μM [α-^{32}P]ATP (0.5 μCi/μL). Reaction products were separated on a 1.2% agarose/formaldehyde gel and revealed by autoradiography. Reaction products are indicated on the *Right* of the gel and radiolabeled 339-nt 3R RNA was used as marker (M) and indicated on the *Left* of the panel. Two reaction products were detected with the unmodified RNA template (lane 2) corresponding to de novo initiation of RNA polymerization and backpriming activity. Chemically 3′-blocked 3R (lane 1) was tested to exclude terminal nucleotide transferase activity and also to prevent backpriming polymerase activity. When using the 3′-end blocked 3R, only the product from de novo initiation polymerization was detected. (*B*) The 7L8/12 complex has comparable polymerase activity on the 3RA or 3R templates. 7L8/12 (500 nM) was incubated for 60 min with 3R or 3RA (500 nM) and a mix of GTP, UTP, and CTP (500 μM each) as well as 50 μM ATP and 0.17 μM [α-^{32}P]ATP (0.5 μCi/μL). Reaction aliquots were quenched by the addition of EDTA/formamide, RNA products were resolved on 20% polyacrylamide/7 M urea gel and visualized by phosphorimaging. ^{32}P-radiolabeled (*) ATP*, ADP*, and AMP* and RNA products are indicated on the *Right* of the autoradiograph.

1. Ackermann M, Padmanabhan R (2001) De novo synthesis of RNA by the dengue virus RNA-dependent RNA polymerase exhibits temperature dependence at the initiation but not elongation phase. *J Biol Chem* 276:39926–39937.

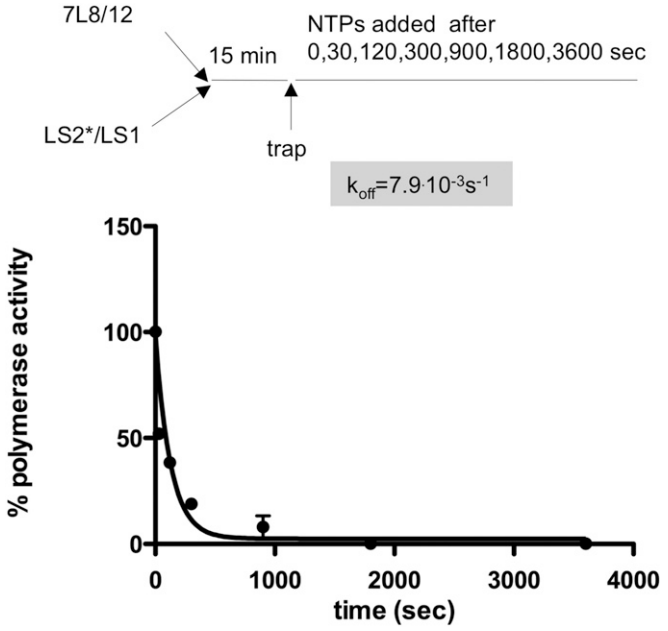

Fig. S5. Determination of the 7L8/12 complex dissociation rate kinetic (k_{off}). Trapping experiment to determine the dissociation rate constant (k_{off}) of 7L8/12 from the LS2/LS1 RNA substrate. 7L8/12 and LS2*/LS1 (the asterisk indicating the position of the ^{32}P label) were preincubated during 15 min at 30 °C to optimize complex formation. Then, either a mix of trap (200-fold excess of cold LS2/LS1) and NTPs (500 μM GTP, ATP, UTP, and CTP) were simultaneously added (defining 100% polymerase activity) or only trap was added, followed at different time points (indicated on the *x* axis) by the addition of NTP mix.

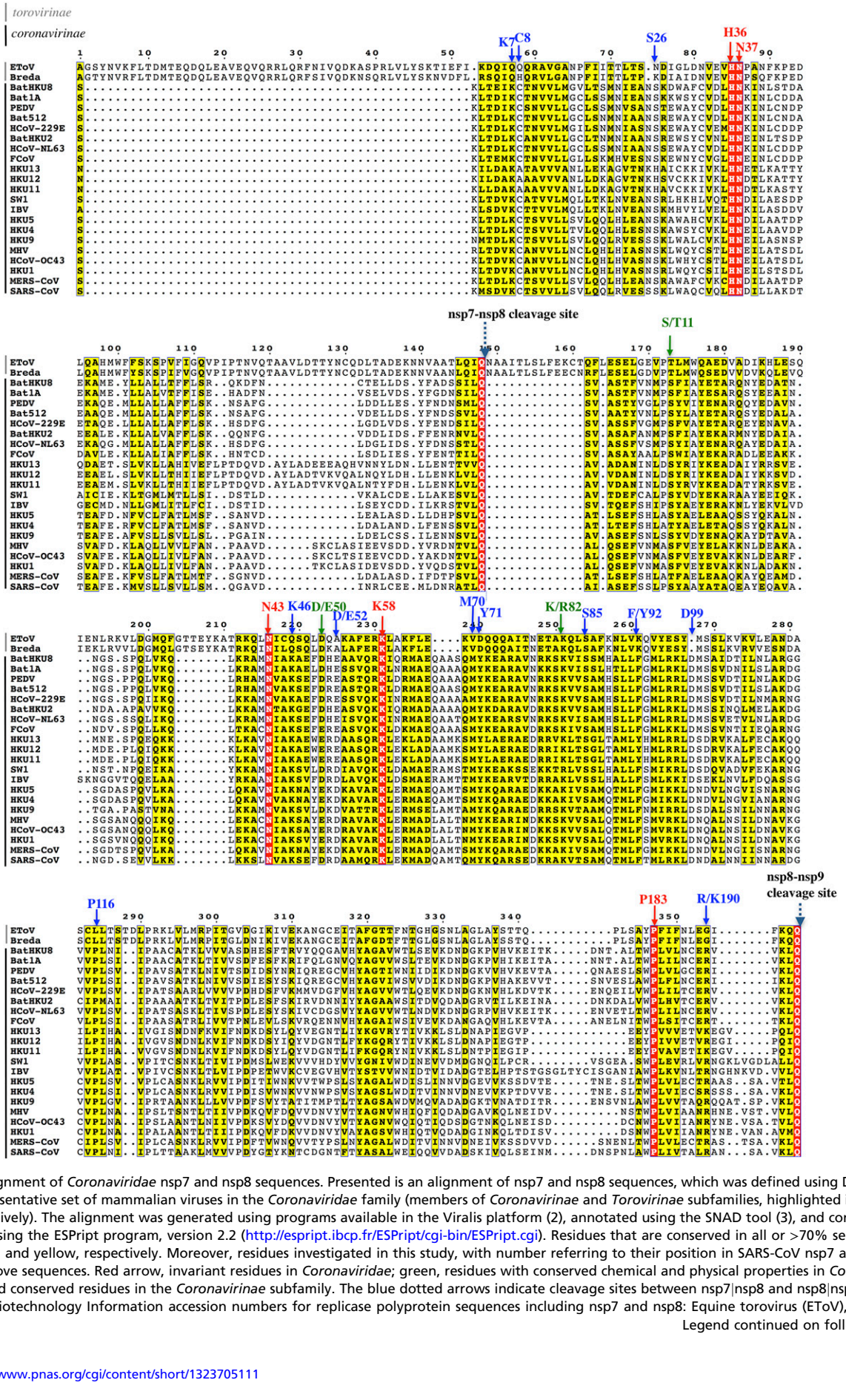

Fig. S6. Alignment of *Coronaviridae* nsp7 and nsp8 sequences. Presented is an alignment of nsp7 and nsp8 sequences, which was defined using DEmARC (1), from a representative set of mammalian viruses in the *Coronaviridae* family (members of *Coronavirinae* and *Torovirinae* subfamilies, highlighted in black and gray, respectively). The alignment was generated using programs available in the Viralis platform (2), annotated using the SNAD tool (3), and converted into this figure using the ESPript program, version 2.2 (http://espript.ibcp.fr/ESPript/cgi-bin/ESPript.cgi). Residues that are conserved in all or >70% sequences are boxed in red and yellow, respectively. Moreover, residues investigated in this study, with number referring to their position in SARS-CoV nsp7 and nsp8 are reported above sequences. Red arrow, invariant residues in *Coronaviridae*; green, residues with conserved chemical and physical properties in *Coronaviridae*; blue, selected conserved residues in the *Coronavirinae* subfamily. The blue dotted arrows indicate cleavage sites between nsp7|nsp8 and nsp8|nsp9. National Center for Biotechnology Information accession numbers for replicase polyprotein sequences including nsp7 and nsp8: Equine torovirus (EToV), DQ310701;

Legend continued on following page

Breda virus (Breda), NC_007447; Miniopterus bat coronavirus HKU8 (BatHKU8), NC_010438; Bat coronavirus 1A (Bat1A), NC_010437; Porcine epidemic diarrhea virus (PEDV), NC_003436; Scotophilus bat coronavirus 512 (Bat512), DQ648858; Human coronavirus 229E (HCoV-229E), NC_002645; Rhinolophus bat coronavirus HKU2 (BatHKU2), NC_009988; Human coronavirus NL63 (HCoV-NL63), DQ445911; Feline coronavirus (FCoV), NC_007025; Munia coronavirus HKU13-3514 (HKU13), NC_011550; Thrush coronavirus HKU12-600 (HKU12), NC_011549; Bulbul coronavirus HKU11-796 (HKU11), NC_011548; Beluga Whale coronavirus SW1 (SW1), EU111742; Infectious bronchitis virus (IBV), NC_001451; Bat coronavirus HKU5-1 (HKU5), EF065509; Bat coronavirus HKU4-1 (HKU4), EF065505; Bat coronavirus HKU9-1 (HKU9), EF065513; Murine hepatitis virus (MHV), AY700211; Human coronavirus OC43 (HCoV-OC43), AY585228; Human coronavirus HKU1 (HKU1), AY884001; MERS-CoV, JX869059; SARS-CoV, AY345988.

1. Lauber C, Gorbalenya AE (2012) Partitioning the genetic diversity of a virus family: Approach and evaluation through a case study of picornaviruses. *J Virol* 86(7):3890–3904.
2. Gorbalenya AE, et al. (2010) Practical application of bioinformatics by the multidisciplinary VIZIER consortium. *Antiviral Res* 87(2):95–110.
3. Sidorov IA, Reshetov DA, Gorbalenya AE (2009) SNAD: Sequence Name Annotation-based Designer. *BMC Bioinformatics* 10:251.

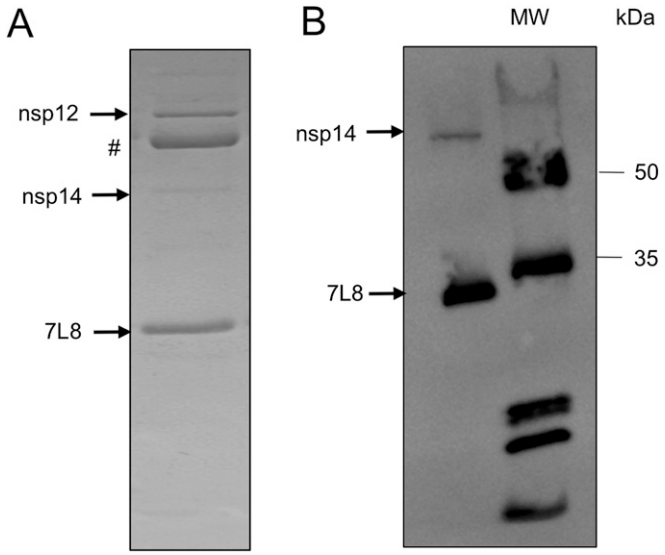

Fig. S7. Purification of 7L8/12 in complex with nsp14 (7L8/12/14). Colysis of *E. coli* cells overexpressing SARS-CoV nsp14 with cells overexpressing 7L8/12 was performed in nsp12 lysis buffer (*Materials and Methods*). Purification of 7L8/12/14 complex was performed in the same buffer as 7L8/12 and consisted of three chromatography steps: (*i*) an IMAC step (elution buffer corresponding to lysis buffer supplemented with 150 mM imidazole); (*ii*) a size exclusion chromatography step (S200 16/60; GE Healthcare); and finally (*iii*) a Strep-Tactin affinity chromatography step (for protein elution, lysis buffer was supplemented with 2.5 mM D-desthiobiotin). (*A*) The 7L8/12/14 complex was purified (see above) and separated by 12% SDS/PAGE and visualized by Coomassie blue staining. #: *E. coli* main contaminant (DnaK, confirmed by MALDI-TOF analysis). (*B*) After the three purification steps, 7L8/12/14 complex was subjected to immunoblotting with an anti–His_5-HRP conjugate to detect the nsp14 and 7L8 hexahistidine-tagged proteins. Molecular weights (MW) are indicated on the *Right* of the panel.

Table S1. Comparison of primer extension activities between copurified polymerase complex 7L8/12 and separately purified nsp7, nsp8, and nsp12

Mutant	7+8+12 primer extension activity, %	7L8/12 primer extension activity, %
Nsp12		
WT	100 ± 9.4	100 ± 5.1
D760A	1.7 ± 3.5	3.5 ± 3.3
Nsp8		
WT	100 ± 9.4	100 ± 5.1
N43A	97.3 ± 8.6	101.6 ± 7.8
D52A	109.5 ± 10.6	96.7 ± 9.9
K58A	30.1 ± 10.5	24.6 ± 4.9
K82A	85.9 ± 12.4	72.5 ± 10.9
P116A	18 ± 5.7	37.1 ± 5.3
R190A	2.4 ± 4.2	3.0 ± 3.0

Five hundred nanomolar 7L8/12 polymerase complex or a mix of nsp12 (500 nM) plus nsp8 (1.5 μM) plus nsp7 (1.5 μM) (named 7+8+12) were preincubated with LS2*/LS1 RNA template (the asterisk indicating the ^{32}P-labeling position) during 15 min at 30 °C, and then 500 μM GTP, CTP, UTP, and ATP were added and incubated 60 min at 30 °C. Quantifications of polymerization products after these 60 min of reaction were made using Image Gauge software. Nsp8 WT either in 7L8/12 context or added to nsp7 and nsp12 separately purified were set up at 100% of polymerase activity. Polymerase activity relative values between 7L8/12 and nsp7 plus nsp8 plus nsp12 WT and mutants are similar. Nsp12(D760A) mutant in the presence of nsp7 and nsp8(WT) and 7L8(WT)/12 (D760A) are shown as negative control. Mutants highlighted in gray indicate important residues for in vitro polymerase activities. Absolute primer conversion rates (at 60 min for WT): 42% ± 4% for 7+8+12; 67% ± 6.3% for 7L8/12. SDs represent the mean of three independent experiments.

Table S2. Overview of SARS-CoV nsp7 and nsp8 mutants and their phenotype

Mutant	Mutation	IF microscopy (nsp4, N), t = 18 h p.t.	Plaque phenotype	Summary of mutant phenotype
Wild type	n.a.	+	WT	WT
Nsp7 K7A	AAG → GCA	+	Small	Crippled
Nsp7 H36A	CAC → GCA	+	Small	Crippled
Nsp7 N37A	AAU → GCA	+/–	Small	Crippled
Nsp8 S11A	UCA → GCU	+	Similar to WT	Similar to WT
Nsp8 N43A	AAU → GCU	+	Similar to WT	Similar to WT
Nsp8 D52A	GAU → GCU	+/–	Small	Crippled
Nsp8 K58A	AAG → GCG	–	No plaques	Nonviable
Nsp8 K82A	AAA → GCA	–	Small	Crippled; rapid pseudoreversion to nsp8-D78N or nsp8-E77T
Nsp8 S85A	AGU → GCA	+	Larger than WT	Similar to WT
Nsp8 D99A	GAU → GCG	+	Small	Crippled
Nsp8 P116A	CCA → GCU	+	Small	Crippled
Nsp8 P183A	CCU → GCA	–	No plaques	Nonviable
Nsp8 R190A	AGA → GCU	–	No plaques	Nonviable

SARS-CoV mutant viruses were launched by transfection of RNA transcripts derived from full-length cDNA clones (two independently produced clones per mutant), as described in *Materials and Methods*. The table lists the mutations introduced and the results of immunofluorescence (IF) microscopy performed on transfected cell cultures after the first round of infection (18 h p.t.), using antibodies recognizing the viral nsp4 and N proteins. Also given is the plaque phenotype of progeny virus harvested at that same time point (see Fig. 5, which also includes growth curves for the most relevant mutants in this study). The white, light gray, and dark gray boxes indicate phenotypes that are similar to WT, crippled, or nonviable, respectively.